

This technique has been improved significantly during the last year. Measurements with 1 percent statistical accuracy in a 10-minute counting time have been reported by the ETH group (6). The limit to dating accuracy will probably be our understanding of sample contamination with "old" and "new" carbon.

A. B. TUCKER

Physics Department, San Jose State University, San Jose, California 95192

W. WOEFELI

G. BONANI

M. SUTER

Laboratory for Nuclear Physics,

Eidgenössische Technische

Hochschule, 8093 Zurich, Switzerland

#### References and Notes

1. F. Swan III, D. Schwartz, Lloyd Cluff, *Bull. Seismol. Soc. Am.* **70** (No. 5) (1980).
2. R. A. Muller, *Science* **196**, 489 (1977).
3. D. Nelson, R. Korteling, W. R. Stott, *ibid.* **198**, 507 (1977).
4. C. L. Bennett, R. P. Beukens, M. R. Clover, H. E. Gove, R. B. Liebert, A. E. Litherland, K. H. Purser, W. E. Sondheim, *ibid.*, p. 508.
5. M. Suter, R. Balzer, G. Bonani, W. Woefli, J. Beer, H. Oeschger, B. Stauffer, *IEEE Trans. Nucl. Sci.* **NS-28**, 1475 (1981).
6. M. Suter, R. Balzer, G. Bonani, W. Woefli, J. Beer, H. Oeschger, B. Stauffer, in *Proceedings of the Symposium on Accelerator Mass Spectrometry* (Argonne National Laboratory, Argonne, Ill., May 1981).
7. Excellent collaboration with J. Beer, H. Oeschger, and B. Stauffer is gratefully acknowledged. This work was supported in part by the Swiss National Science Foundation, the U.S. Geological Survey Earthquake Hazards Reduction Program, and Chevron Oil Field Research Company.

17 May 1982

## East Pacific Rise Near 13°N:

### Geology of New Hydrothermal Fields

**Abstract.** *Abundant massive sulfide deposits are present at the crest of the East Pacific Rise near 13° North, where the opening rate is about 12 centimeters per year. Large manganese and helium-3 anomalies in seawater samples, evidence of intense present-day activity of hydrothermal springs, indicate that sulfides are still being produced along this segment of the rise. Massive sulfides also occur on adjacent off-axis seamounts.*

The most detailed studies of the East Pacific Rise have been concentrated on a segment of the rise crest near 21°N (1, 2), where the opening rate is 6.2 cm/year (3). The first find of polymetallic sulfide deposits on the East Pacific Rise was made there (4). A later investigation led to the discovery of active, sulfide-producing hydrothermal vents and associated fauna (2). We report results of exploratory work in May and June 1981 with the R.V. *Charcot* on a segment of the East Pacific Rise which is about 1000 km to the south of the 21°N area and where the spreading rate is about twice as fast. The cruise, "Clipperton," was designed to prepare the way for a submersible operation in 1982. The main area selected for detailed investigation (zone A) lies about halfway between the two fracture zones, Orozco and Clipperton, where high <sup>3</sup>He and manganese (5, 6) anomalies in deep water were previously found (Fig. 1).

The 400-km-long segment of the East Pacific Rise between the Orozco (15°N) and Clipperton (10°N) fracture zones has a narrow horstlike crest; it is apparently linear for long distances and has a low, along-strike relief, the depth at the rise axis varying between about 2700 and 2500 m (Fig. 1). The relatively flat zero-age bathymetric pattern may reflect a correspondingly consistent crustal thickness. A single-channel seismic reflection profile, made while navigating according

to the real-time Seabeam plot precisely along the topographic axis of the rise between 12°52'N and 12°N, shows an intermittent reflection at a nearly unvarying depth corresponding to a 0.6-second double travel time below the sea floor. It is not known whether the reflector is real or is a side echo from sea-floor relief parallel to the rise axis.

Zone A, lying between 12°38'N and 12°54'N and between 103°49'W and 104°01'W, covers about 600 km<sup>2</sup> (Fig. 1). The rise crest strikes north 345° and its axial zone is about 1500 m wide. Along much of its length, it incorporates a

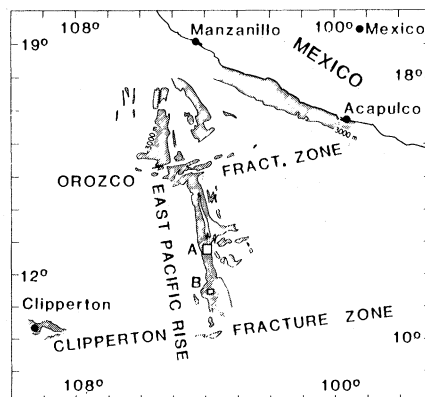


Fig. 1. Locations of the principal study area near 12°50'N (zone A) and the secondary study area near 11°30'N (zone B). Shading indicates depths less than 3000 m. [Courtesy of J. Mammerickx]

double ridge system with a steep-sided central graben less than 40 m deep and a maximum depth below sea level of 2465 m. The western side of the axial zone is characterized by narrow, linear, steplike ridges with steep inward-facing scarps, which are the hallmark of the "normal" tectonics associated with accretion at the rise crest. On the eastern side this structural grain, where it exists, stops 3 km out from the axis; beyond this the morphology is determined by the presence of two seamounts, both about 2 km from the rise axis and about 250 m above the surrounding sea floor (Figs. 1 and 2A). The northern seamount has a broader, flatter top and gentler upper slopes. The seamounts may have been created by off-axis volcanism in approximately their present location or may have been the sites of renewed eruptive activity of smaller volcanoes originally closer to the axis. A third seamount, rising about 1000 m above the surrounding floor, was discovered outside the main study area, about 18 km west of the axial zone near 12°34'N and 104°02'W. We named this the Clipperton seamount.

Color photographs of the sea floor in the zone A axial area, taken with a deep-tow system over a total distance of about 35 km, show that the flanking scarps of the graben are commonly associated with talus piles that may produce local relief as great as 20 m. They also show numerous, en echelon, open fissures in the very lightly sedimented central graben. The fissures are oriented parallel to the regional strike of the rise crest and are between a few tens of centimeters and about 4 m wide. Some fissures are present on the bordering ridges where interconnecting pockets of sediment occur and the fissures also strike parallel to the rise axis. The photographs show the presence of the three main categories of lava flows previously recognized on the East Pacific Rise (1, 7). Lobate sheet flows are the most abundant and occur in the central graben and on the lateral highs (Fig. 2B). Unbroken flat sheet flows, apparently less than 1 m thick, are found in isolated patches, but their associated debris occurs everywhere, particularly in the central graben. The passage from lobate to flat sheet flows is generally transitional so that clear boundaries cannot be easily drawn. Pillow flows are prominent on the slopes of the twin ridges bordering the central graben, particularly where the sediment cover is greatest. The pillows often sit on, or are in lateral contact with, lobate flows from which they cannot be readily distinguished and appear to be derived. It has been suggested (8) that sheet flows rep-

resent early, highly productive volcanic events while pillow flows occur during the slowing down of volcanic activity. In any event, the sheet flows are more prominent than pillow flows in the central graben, where many vertical pillars, remnants of the original lava lakes, stand up to 10 m or more above the surrounding floor.

The floor of the central graben is also the principal setting of colored deposits that resemble the massive sulfides of the type previously seen and sampled by submersible in the 21°N area of the rise (4). About 30 sites can be identified in the photographs by their "scoria-like" appearance, by the presence of small circular orifices, and by their variegated colors (Fig. 2B). Green and reddish brown patches are often encountered in areas with unsorted, large debris mixed with powdery looking deposits. Locally, numerous deep yellow spots are observed in these sulfide-rich sites. Yellow spots, presumably sulfates, are also seen along narrow fissures in flat basaltic flows. In some cases, the deposits may

have the form of the moundlike edifices of the 21°N type (4). Identification of the colored deposits as sulfides was supported by dredging.

Basaltic pillows and sheet flows were recovered at 17 stations, some by transponder-navigated rock dredges, others inadvertently by the deep-towed camera system (Fig. 2). Samples of fresh basaltic glass with very thin manganese coatings were collected from the axial zone, from the southeast seamount, and from the Clipperton seamount. The samples were grouped into three main categories according to the order of crystallization of the major mineral phases and the TiO<sub>2</sub> content and FeO/MgO ratio of their glassy margins. The olivine basalts, found mainly at the rise crest (DR1 and DR4 in Fig. 2A), have olivine, with or without plagioclase, as the primary phase. The TiO<sub>2</sub> content is 1.1 to 1.6 percent and FeO/MgO is 1 to 1.5. The least fractionated basalt (low TiO<sub>2</sub> and FeO/MgO) contains olivine with 88.2 percent forsterite. The plagioclase-olivine-pyroxene basalts occur both at the

rise axis and off-axis (DR1 and DR4 in Fig. 2A). Chemical analyses of these samples indicate a relatively high TiO<sub>2</sub> content (1.4 to 2.1 percent) with respect to the olivine basalts and a lower forsterite content of the olivine (generally less than 83 to 86 percent forsterite). Plagioclase-rich basalts were recovered only from the Clipperton seamount. They are porphyritic, with more than 20 percent (by volume) of plagioclase. Bulk rock analyses indicate a low TiO<sub>2</sub> content (< 1 percent). On the basis of TiO<sub>2</sub> content and FeO/MgO ratios, the rocks recovered from the 13°N area have wider range of composition and tend to be more fractionated than those collected from the East Pacific Rise at 21°N, where the opening rate (6 cm/year) is about half as fast.

The metalliferous deposits we recovered include a sulfide sample from the axial zone of the rise, sulfides and oxides from the southeastern off-axis seamount, and sulfides and manganese oxides from the Clipperton seamount. The sulfide sample from the axial zone comes from

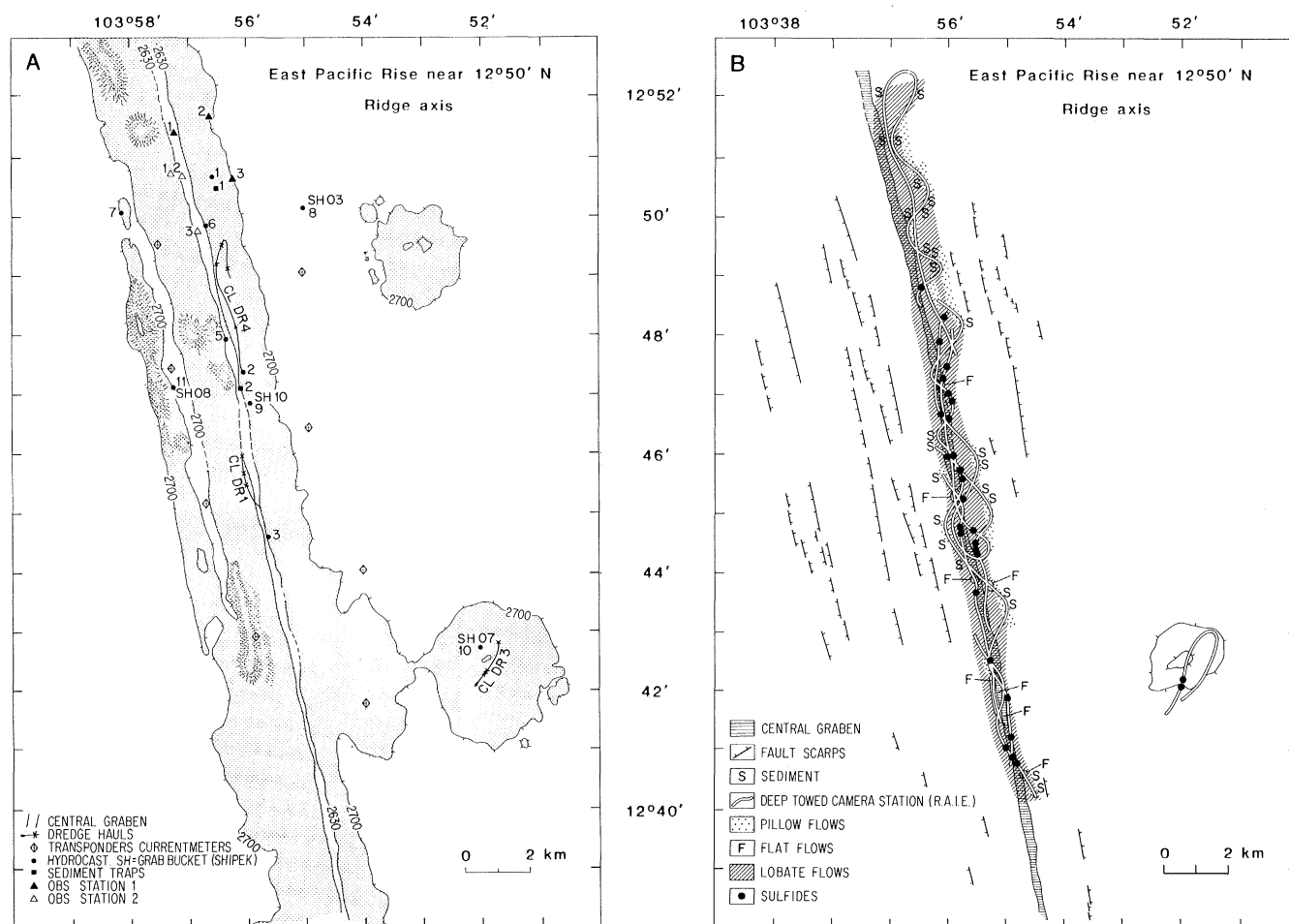


Fig. 2. (A) Sketch diagram of the crestal area of the East Pacific Rise in zone A shallower than 2700 m (stippled), showing the central graben (dense stippling) and the locations of the stations occupied. Crosses on dredging tracks indicate hits. Prominent isolated peaks and ridges are indicated by hachuring. (B) Schematic representation of the surface geology in zone A based on the bathymetry and on deep-towed photographic coverage (RAIE stations).

the southern portion of the area. It is dark in color and made up essentially of wurtzite (with rare chalcopyrite inclusions) and scattered small idiomorphic pyrite and marcasite crystals. Numerous circular, interconnecting tubes (about 1 cm in diameter) are present. The tube walls consist of concentric lamellae of opal alternating with sulfide minerals similar to those described from the 21°N area on the East Pacific Rise (9-11). Bulk analyses of some trace elements by atomic absorption spectrometry show local presence of silver (22 ppm) and cadmium (236 ppm).

The metalliferous fragments from the southeastern seamount were dredged from near the summit together with basaltic rocks (DR3 in Fig. 2A). They consist of both fresh and altered products and include massive sulfides, silica-rich sulfides, and highly oxidized samples. The massive sulfides are compact with sporadic tubular cavities and, locally, thin coatings of Fe-Mn oxides. They are made up of well-crystallized pyrite and marcasite, sometimes associated with copper sulfides (chalcopyrite and covellite). Zinc sulfides occur as minor constituents, forming small patches or hexagonal inclusions (wurtzite) scattered in the iron sulfide phases. Association of iron sulfides with barite is observed in some of the samples. The crystals of barite are identical to those encountered in the deposits from the East Pacific Rise near 21°N (9).

The silica-rich sulfides have a scoria-like appearance with sporadic tubular cavities. They consist primarily of pyrite and marcasite, accompanied by minor copper and zinc sulfides. The sulfide phases lie in a dark gray, compact matrix made up of hydrated amorphous silica (opal). Numerous well-crystallized framboidal pyrites are observed among the sulfide crystals scattered in the massive opal. Very small spots of cobalt-rich pyrite are present in silica-rich sample DR3-6 (microprobe analysis shows up to 17 percent cobalt by weight). The highly oxidized samples are soft, friable, orange to brownish red, and composed primarily of iron oxides and hydroxides (goethite and limonite). Amorphous manganese products are also present. Traces of sulfides that may represent degradation of massive sulfides are found throughout the samples. Alteration products, principally sulfates, are often observed as patches on the surface. Some of these phases are similar to those described from 21°N on the East Pacific Rise.

The small sulfide and manganese oxide fragments found among the dredged basalts from the Clipperton seamount

are dark and massive. They differ from the thin coatings of manganese oxide observed locally on some sulfide samples in that they represent portions of thick (3 to 4 cm) self-supporting crusts. Microscopically, they show a colloidal appearance with well-developed spheroidal textures. Considering the crustal age in the sampling area (about 300,000 years, assuming an average half spreading rate of 6.2 cm/year), the thickest Fe-Mn accumulation suggests proximate discharge of hydrothermal fluids.

Sediments were sampled with a piston corer or grab at seven stations west of the axis, along a line out to about 77 km near 12°34'N. The sediments, collected between depths of 2890 and 3250 m, consist of a dark brown fraction intermixed with 3 to 35 percent sand-size grains (> 63  $\mu$ m). The coarser fractions consist of carbonaceous and siliceous organisms, basaltic glass, plagioclase, olivine, and Fe-Mn microconcretions. The fine fraction (< 63  $\mu$ m) shows high concentrations of iron (6 to 11 percent) and manganese (1 to 3 percent) and an aluminum content of about 3 to 7 percent. The Fe/Mn ratio increases with distance from axis and the highest manganese concentrations are usually found near and on the ridge axis. A sediment trap (12) designed to recover suspended particles from seawater was moored for 10 days at the rise crest [about 50 m above the sea floor and about 300 m east of the axis (station 1 in Fig. 2A)].

About 120 mg of material consisting of foraminiferal tests, pteropods, fecal pellets, organic aggregates, and inorganic fractions were recovered. Among the inorganic precipitates are iron oxides and sulfides and small unidentified crystals.

The pattern of transport of the suspended material was investigated with 33 moored current meters in zone A; 19 of the meters were left close to the sea floor for 5 to 10 days and the other 14 were lowered and raised during the hydro-cast stations in order to have complementary information at these sites. The 19 meters were attached to the bottom-moored transponders used for navigation at a maximum height of 200 m above the sea floor. Sixteen functioned correctly and gave information about the current vectors on both sides of the rise axis (Fig. 2A). The progressive vector diagrams that were obtained suggest two principal phenomena: (i) a semidiurnal periodicity, with current directions tending to be controlled by the geometry of the major structures of the sea floor, and (ii) a general tendency of the current to be directed westward at an average speed of

5 cm/sec. The maximum current speed measured in zone A was a surprisingly high 10 cm/sec.

The general westerly direction of the deepwater bottom current is supported by the results of a study of manganese and <sup>3</sup>He plumes. Fourteen hydro-cast stations were occupied during the cruise. Twelve of these were in zone A and showed manganese anomalies in the lower 100 to 150 m of the water column (Fig. 2A). The maximum peaks occurred 150 m above the sea floor in the northern part of the area. Eight hydro-cast stations were concentrated in the axial area of the rise, and three of them showed concentrations of manganese and increments of <sup>3</sup>He as high as (30 to 36)  $\times 10^{-9}$  mole/kg and 73 percent, respectively (5). Four lowerings were made off-axis, at about 2 km on each side of the axial zone, to test whether there is a preferential direction of transport of manganese away from the crest (Fig. 2A). No major manganese anomalies were detected on the eastern side of the rise axis. However, a small anomaly (< 15  $\times 10^{-9}$  mole/kg) was detected in the bottom water sampled near the summit of the southeastern seamount. The two hydro-cast stations located west of the rise axis showed high manganese concentrations in the near-bottom water.

In summary, the most recent volcanic activity in the principal study area (near 13°N), as indicated by the freshest flows and least sediment cover, occurs mainly in a faulted axial valley less than 500 m wide and about 35 m below the level of the bordering ridges. On the basis of previous experience, we consider the colored deposits evident in our large collection of sea-floor photographs to be unambiguous evidence of metalliferous sulfide deposition in the central valley. Dredge hauls show that the deposits include zinc-rich sulfides of the type previously sampled at 21°N and on the Galápagos spreading center. Manganese and helium anomalies in the water column indicate the presence of high-temperature hydrothermal springs, particularly in the northern part of the study area. Three new off-axis seamounts were discovered: two small volcanoes about 8 km east of the rise axis in the main study area (zone A) and one large volcano about 18 km west of the axis. The southeastern seamount is the site of iron- and silica-rich sulfides and highly oxidized material (gossan).

Inasmuch as there are very abundant sulfide deposits in the 13°N area, our findings support the view that the Galápagos and 21°N areas are not unusual and that direct evidence of intense hy-

drothermal venting and associated metalliferous deposits should be sought all along the East Pacific Rise. The 13°N area differs morphologically from the 21°N area, where the spreading rate is about half as fast. It will now be important to establish the distribution of hydrothermal activity between fracture zones. We briefly investigated a second area of the axial zone (zone B, near 11°30'N) along the rise segment between the Orozco and Clipperton fracture zones and found indications of hydrothermal activity from hydrocasts and sea-floor photographs. Finally, the presence of massive sulfides on off-axis seamounts opens an interesting field for further exploration.

R. HEKINIAN

Centre Océanologique de Bretagne,  
29273 Brest Cédex, France

M. FEVRIER

Centre Océanologique de Bretagne  
and Département de Géologie,  
Université de Bretagne Occidentale,  
29283 Brest Cédex, France

F. AVEDIK

P. CAMBON

J. L. CHARLOU

H. D. NEEDHAM

J. RAILLARD

Centre Océanologique de Bretagne

J. BOULEGUE

Université de Paris 6 et 7,  
75230 Paris Cédex 05, France

L. MERLIVAT

DPC-CEN Saclay,  
91191 Gif-sur-Yvette Cédex, France

A. MOINET

Université de Paris 6 et 7

S. MANGANINI

Woods Hole Oceanographic Institution,  
Woods Hole, Massachusetts 02543

J. LANGE

Preussag Aktiengesellschaft,  
3000 Hannover,  
Federal Republic of Germany

tain G. Paquet and the officers and crew of the R.V. *Jean Charcot* for the skillful handling of the wide range of equipment used during the cruise. We thank J. Legrand, M. Lehaitre, and G. Vincent for operating the deep-towed camera system RAIE; J. C. Cavarec for handling the bottom-moored transponder navigational system; and J. L. Reaute, A. Le Bot, and A. Gourmelon for acquisition of the multichannel narrow-beam echo sounder (Seabeam) data. R.

Conogan and J. Roudaut assisted in handling the seismic reflection gear. G. Floch was responsible for the rock inventory and thin sections on board. Final maps were prepared by D. Carre, A. Grotte, and S. Monti. M. Bohn performed the microprobe analysis of the samples and S. Marques and R. Kerbrat screened the sediment samples for examination and chemical analysis.

19 July 1982; revised 16 November 1982

## Controlled Stimulation of Magnetospheric Electrons by Radio Waves: Experimental Model for Lightning Effects

**Abstract.** Magnetospheric electrons precipitated by ground-based coded very low frequency radio transmissions have been detected by rocket measurement of bremsstrahlung x-rays, caused by impact of the electrons with the upper atmosphere. The direct correlations obtained between the very low frequency signals and the x-rays demonstrate the limits of sensitivity required and indicate that this remote sensing technique would be useful for future study of very low frequency effects induced by single lightning strokes.

Recent interest in influences of human activities on the upper terrestrial environment has centered on radio wave stimulation of plasma-wave instabilities in the magnetosphere (1). The magnetosphere is the outermost portion of the near-earth environment and is regulated by interaction between the earth's and interplanetary plasmas and magnetic fields. Two principal anthropogenic sources of radio wave noise are thought to arise from power lines (2) and high-powered very low frequency (VLF) transmitters (3, 4), although serious doubts have been raised about the magnitude of the effect from power lines (5). Theoretical studies (4, 6) imply that the radio waves should trigger the precipitation of energetic electrons from the trapped particle belts in the earth's magnetosphere.

Before now, direct experimental verification of the occurrence of transmitter-induced electron precipitation has not

been obtained (4). Indirect evidence has been offered in the form of narrow peaks observed in the energy spectra of precipitating electrons linked with VLF transmitter signals (7), satellite-based observations of emission triggering by VLF transmitters (8), and low-latitude energetic (> 100 keV) electron precipitation linked to Soviet transmitters (9). In addition, fluctuations in ground-based riometer records have been attributed to ionospheric modulations caused by VLF-induced electron precipitation from Siple Station, Antarctica (10), and perturbations in propagating signals from transmitters in the Northern Hemisphere have been linked to enhanced ionization from electron precipitation at the ends of field lines (11). This indirect evidence combined with recent theoretical results provided the motivation for the experiment described here. Finally, it should be noted that for natural VLF sources, possible correlations between particle

### References and Notes

1. Cyamex Scientific Team, *Mar. Geophys. Res.* **4**, 345 (1981).
2. RISE Project Group, *Science* **207**, 1421 (1980).
3. R. L. Larson, *Bull. Geol. Am.* **82**, 823 (1971).
4. Cyamex Scientific Team and H. Bougault, P. Cambon, R. Hekinian, *Nature (London)* **277**, 5601 (1979).
5. L. Merlivat, J. Boulegue, B. Dimon, *Eos* **62**, 913 (1981).
6. J. Francheteau, abstract of paper presented at the American Geophysical Union Chapman Conference, Warrenton, Va., 1981.
7. R. D. Ballard, J. Francheteau, T. Juteau, C. Rangin, W. Normark, *Earth Planet. Sci. Lett.* **55**, 1 (1981).
8. R. D. Ballard, R. T. Holcomb, T. H. Van Andel, *J. Geophys. Res.* **84**, 5407 (1979).
9. M. Fevrier, thesis, Université de Bretagne Occidentale and Centre Océanologique de Bretagne, Brest, France (1981).
10. M. M. Styr et al., *Earth Planet. Sci. Lett.* **53**, 382 (1981).
11. R. M. Haymon and M. Kastner, *ibid.*, p. 363.
12. S. Honjo and J. F. Cannell, *Woods Hole Oceanogr. Inst. Tech. Rep. WHOI-79-80* (1979).
13. The Clipperton cruise was carried out as part of the CNEXO program for the study of ocean floor hydrothermalism. We are grateful to Cap-

Table 1. Rocket flight and range logistics.

Datum	Rocket	
	31.030	31.031
	<i>Time</i>	
Date	23 June 1982	7 July 1982
Launch ( $T_0$ )	1540 UT (day)	0901 UT (night)
Apogee	$T_0 + 148.9$ sec	$T_0 + 144.9$ sec
	<i>Altitude</i>	
Apogee	84.8 km	80.0 km
$T_0 + 300$ sec	49.4 km	48.1 km
$T_0 + 540$ sec	34.3 km	33.9 km
	<i>Transmitter time</i>	
On	1539 UT	0900 UT
Off	1549 UT	0910 UT
	<i>Range coordinates</i>	
Position	37.9°N, 75.5°W	37.9°N, 75.5°W
Magnetic $L$ value	2.60	2.60
	<i>Transmitter coordinates</i>	
Position	39.0°N, 76.5°W	39.0°N, 76.5°W
Magnetic $L$ value	2.76	2.74